Supplementary Information for Probing Excitons, Trions and Dark Excitons in Monolayer WS_2 using Resonance Raman Spectroscopy

Experimental Details

AUTHOR NAMES Liam P. McDonnell[1], Chung-Che Huang[2], Qingsong Cui[2], Dan W. Hewak[2], David C. Smith[1]*

AUTHOR ADDRESSES. [1] School of Physics and Astronomy, University of Southampton, Southampton SO17 1BJ, United Kingdom.[2] Optoelectronic Research Centre, University of Southampton SO17 1BJ, United Kingdom.

Measurements on Multiple WS_2 Flakes

To ensure the resonance Raman profiles were reproducible we performed measurements on two separate flakes grown on the same substrate. Both flakes are shown in Figure S1 (a-b). The resonance Raman profiles were obtained at 4K and 295K using the same excitation energies as stated in the main paper. At 4K, as shown in Figure S1c, there is clear agreement between the two resonance profiles. In the case of the measurements at 295K the obtained resonance profiles are both centered at similar energies although there is a slight variation in resonance width with extension towards higher energies on the second flake. Fitting of the resonance profiles and comparing the values obtained on samples S1 and S2 shows for the 4K datasets that the fitted coefficients are in agreement to within the error obtained from the fitting. In the case of the 295K results the fitting parameters are all within experimental error for the two samples apart from the exciton energy which differs by approximately 4 times the error. We believe this difference is due to underlying sample differences and in no way invalidates the underlying model we discuss in the main manuscript. The fitted resonance profiles for the A_1' and E' at 4K and the A_1' at 295K are shown in Figure S2, and the fitted coefficients for the A_1' at 4K and 295K are presented in Table S1 and S2 respectively. We also present the fitted amplitude coefficients for the E' alongside the ratio of the E'/A_1' on S1 and S2 for the 4K datasets in Table S3.

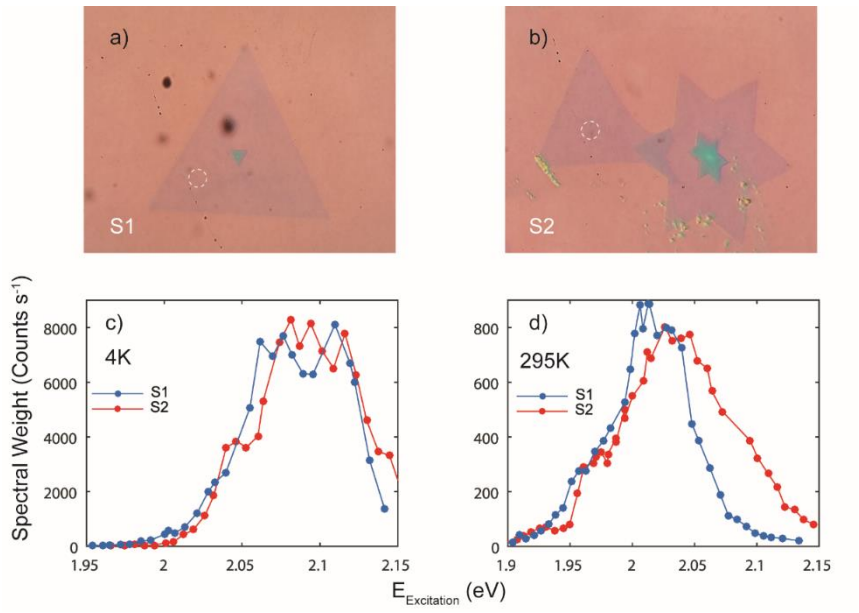

Figure S1 *(a-b) Optical microscope images of the monolayer WS_2 flakes used for resonance Raman measurements denoted as S1 and S2 respectively. The results presented in the main paper were from measurements on S1 (a). c-d) Resonance Raman profiles obtained for the A1' mode on both samples S1 and S2 at 4K and 295K respectively.*

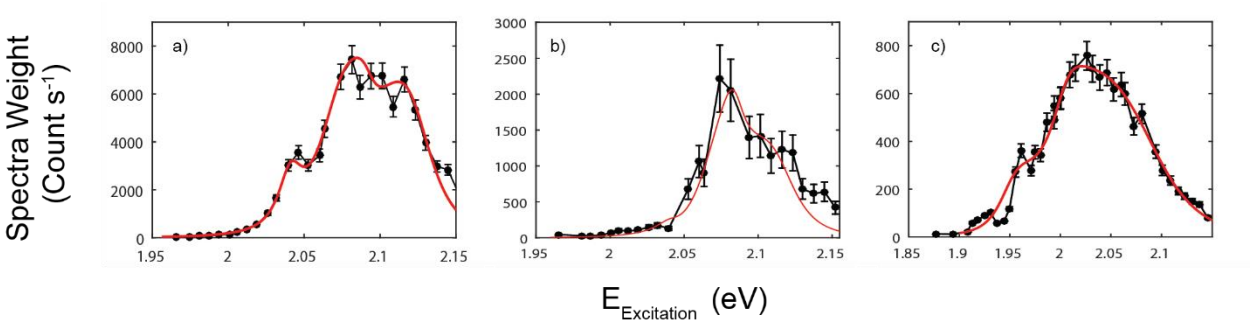

Figure S2 *Resonance Raman profiles obtained from repeat measurements on flake S2 where (a-b) correspond to the A_1' and E' resonance profiles obtained at 4K, and (c) the A_1' resonance profile obtained at 295K. Error bars correspond to the experimental error determined from repeat measurements throughout the experimental run.*

Table S1 *Comparison of fitted amplitudes, linewidths and energies for A_1' resonance Raman profiles taken at 4K on samples S1 and S2. Errors shown for the fitted coefficients correspond to one standard deviation and were obtained from the fitted model. The units of the amplitude coefficients are* $10^{-3}\sqrt{Counts\ s^{-1}} \cdot eV^2$

	XX	XX^-	X^-X^-	E_X (eV)	Γ_X (eV)	E_{X^-}(eV)	Γ_{X^-}(eV)
S1	88.1±2.2	21.4±1.9	70.6±2.8	2.064±0.001	0.018±0.004	2.038±0.006	0.027±0.008
S2	82.9±1.7	40.3±1.8	72.9±2.0	2.070±0.011	0.023±0.02	2.041±0.004	0.010±0.006

Table S2 *Comparison of fitted coefficients for A_1' resonance profiles obtained on S1 and S2 at Room Temperature. Errors shown for the fitted coefficients correspond to one standard deviation and were obtained from the fitted model. Units of the amplitude coefficients are as* $10^{-3}\sqrt{Counts\ s^{-1}} \cdot eV^2$

	XX	XX^-	X^-X^-	E_X (eV)	Γ_X (eV)	E_{X^-}(eV)	Γ_{X^-}(eV)
S1	58.54±0.62	2.83±0.70	3.43±0.79	1.989±0.002	0.036±0.003	1.944±0.004	0.011±0.003
S2	121.77±51.11	42.08±13.84	34.06±12.48	2.036±0.011	0.066±0.013	1.951±0.005	0.025±0.005

Table S3 *Presents the fitted amplitude components for the E' phonon at 4K on sample S1 and S2 and the ratios of E'/ A_1' phonon amplitudes. Errors shown for the fitted coefficients correspond to one standard deviation and were obtained from the fitted model. Units for the amplitude coefficients are given as* $10^{-3}\sqrt{Counts\ s^{-1}} \cdot eV^2$

Raman Channel	E'			Ratio E'/ A_1'		
	XX	XX^-	X^-X^-	XX	XX^-	X^-X^-
S1	31.7±1.3	7.52±1.1	24.0±1.7	0.359±0.018	0.351±0.060	0.341±0.028
S2	33.4±2.7	12.1±2.1	21.1±3.6	0.403±0.011	0.300±0.022	0.290±0.016

Raman Peak Assignment – Dispersion Relation Comparison

Theoretical predictions for phonon frequencies in monolayer WS_2 data were extracted from results presented in Sanchez et al and Berkdemir et al [19, 27]. The predictions were compared to the experimental values of Raman peaks corresponding to the A_1', E' and LA. The best agreement was with the results of Berkdemir *et al*. The assignment of the unassigned peak was then carried out using the Berkdemir predictions for phonon frequencies. The possible two phonon combination mode frequencies are presented in Table S4 and Table S5 for the M and K points respectively. The experimentally determined values for the unassigned peak relative to the Si peak at 520cm^{-1} is 479.0cm^{-1}. Therefore the closest combination mode is the E'' (LO1)(M)+TA(M) phonon.

Table S4 *Predicted Raman shifts for combination modes occurring due to M point phonons obtained using data extracted from Berkdemir et al.*

Phonon Combination Modes	Predicted Raman Shift (cm^{-1})
2LA	358.0
E''(TO1)+TA	452.4
E''(TO1)+ZA	462.9
E'(TO2)+TA	473.3
E''(LO1)+TA	478.2
E'(TO2)+ZA	483.8
E''(LO1)+ZA	488.6
E'(LO2)+TA	498.3
E'(LO2)+ZA	508.8

Table S5 *Predicted Raman shifts for combination modes occurring due to K point phonons obtained using data extracted from Berkdemir et al.*

Phonon Combination Modes	Predicted Raman Shift (cm^{-1})
2LA	372.0
E''(TO1)+ZA	482.2
E''(TO1)+TA	482.2
E'(TO2)+ZA	495.1
E'(TO2)+TA	495.1
E''(LO1)+ZA	499.1
E''(LO1)+TA	499.1
E'(LO2)+ZA	503.1
E'(LO2)+TA	503.1

Linear Power Dependence

The power dependence of the Raman intensity was measured at both 4K and 295K with an excitation energy of 2.016eV, which corresponds predominantly to the lower energy excitation reported in the main paper. The obtained spectra as a function of power were fitted to obtain the Raman intensity of the A_1' peak and are shown in Figure S3 (a-b). The results of this clearly show a linear relationship at both 4K and 295K. As discussed in the main body of the paper, this is indicative of the low energy excitation being attributed to trions and not biexcitons. In addition we present the Raman spectra obtained for power linearity at 4K which have been background subtracted and normalized Figure S3c, and show no significant variation in the width or position of the A_1' peak as a function of excitation power.

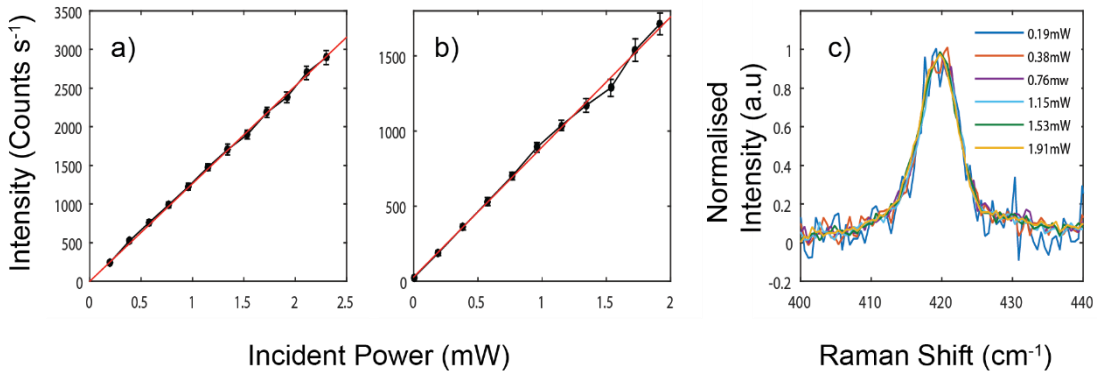

Figure S3 *Raman intensity of the A_1' mode was measured as a function of power at 4K (a) and 295K (b) with a linear fit applied to both sets of data, which is shown by the red line error-bars shown are 95% confidence bounds obtained from fitting Raman peaks. (c) Raman spectra obtained at 4K as a function of power background subtraction has been performed and spectra normalized using the fitted peak amplitudes.*

Anti-Stokes/Stokes Temperature Measurements

To determine the true sample temperature during the experiments anti-Stokes and Stokes Raman spectra were measured with the laser tuned to the peak of the WS_2 resonance as a function of excitation power. The Raman spectra were corrected for the efficiency of the spectrometer. The intensity of the Raman peaks were obtained by fitting Lorentzian line shapes and these were corrected for the reflectivity of the sample. The ratio of the anti-Stokes and Stokes Raman intensities are related to the temperature by the following equation for the case of non-resonant excitation [S1]:

$$\frac{I_{As}}{I_S} = \frac{(v_l + v_{ph})^3}{(v_l - v_{ph})^3} e^{-\frac{hv_{ph}}{k_b T}}$$

Resonance effects will lead to a multiplicative correction to the non-resonant ratio which varies only slowly with temperature[S2].

Measurements were initially taken at 4K with an incident laser power of 1mW and 2mW on the WS_2 and Si substrate respectively. Whilst we obtain significant Stokes signal in a 1 min exposure, 2.82×10^5 counts at the maximum of the 417cm^{-1} peak, we are unable to detect any anti-Stokes scattering above the noise with a 30 min exposure. Based on the observed intensity of the Stokes signal and the noise on the anti-Stokes spectra we can constrain the temperature of the sample to be below 42K. In order to be able to constrain the temperature to a value of 20K would require an exposure time of the order 10^9 longer which is not experimentally possible.

Measurements of the temperatures obtained from the anti-Stokes to Stokes ration for the Si (520 cm^{-1}) peak and the WS_2 A_1' (417 cm^{-1}) peak at 150K and 295K are shown in Figure S4 (a-b). The temperatures obtained for the Si substrate are in agreement with the temperature obtained from the cryostat sensor to within 3K and are independent of incident laser intensity. For the WS_2 measurements resonance effects means that the ratio of anti-Stokes to Stokes scattering depends on excitation wavelength. Application of the non-resonant expression above to the raw, uncorrected anti-Stokes to Stokes ratios gives a WS_2 temperature of 132K and 182K at 150K and 295K respectively. To correct for the resonance effects we adjusted the anti-Stokes to Stokes ratios by a single scaling factor at each temperature which is chosen so that the intercept of a linear regression fit to the obtained temperatures versus excitation intensity is the same as the cryostat sensor temperature. This process would in no way prevent us from observing any laser induced heating. Based upon the measurements we can place a quantitative upper limit on laser induced heating of 3K or less at 150K and 295K. There is no evidence of laser heating of the sample at any temperature and so we can assume that the cryostat sensor temperature can be used as a good measurement of the sample temperature.

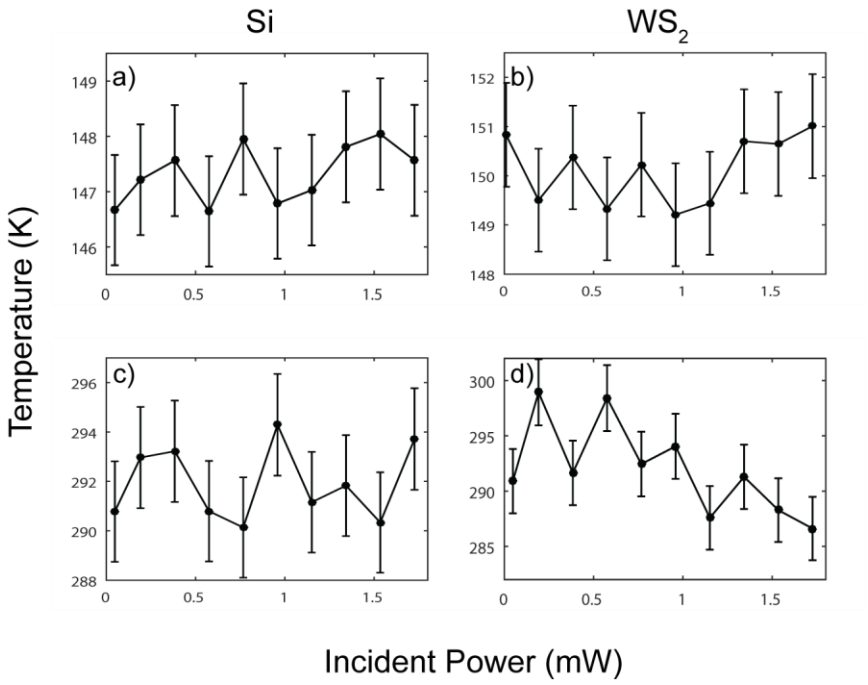

Figure S4 *Power dependence of the sample temperature obtained from Anti-stokes and Stokes Raman measurements at 150K (a-b) and 295K (c-d) on Si substrate and WS_2 spectra respectively. The laser wavelength was tuned to peak of the resonance profile fits presented in main paper, i.e. 603.95nm and 623.50nm at 150K and 295K respectively.*

Micro-reflectivity and Raman Enhancement Factor

For the case of monolayer materials prepared onto non-transparent substrates, the layered nature of the system leads to optical interference effects. The effect of the interference on the Raman scattering amplitude is well known and methods to correct for this effect have been presented in Yoon *et al*. and Zhang *et al.* [S3, S4]. This requires the calculation of a Raman Enhancement Factor (REF) of the form shown in eq(1):

$$\int_0^d |E_{Ab}(x)E_{Sc}(x)|^2\, dx$$

Where E_{ab} and E_{sc} are the electric field strength at the absorbed and scattered wavelengths respectively and *x* defines the position inside the monolayer. The electric field strength is determined by modelling the reflectivity spectra of WS_2. T matrix calculations are then performed using the known refractive indices of the SiO_2 and Si layers [S5, S6]. The dielectric response of WS_2 is then modelled using three Lorentzian oscillators, which have been shown to dominate the optical response of WS_2 by Li et al 2014 [S7]. The micro-reflectivity measurements were carried out using a tungsten halogen lamp and a fiber coupled Ocean Optics HR4000 USB spectrometer with a protected silver mirror as a reference signal. The reflectivity measurements were obtained at 4K and 295K to account for any temperature dependent effects. The spectra were then fitted and the REFs obtained: these results are shown in Figure S5 (a-b). It is clear that the temperature dependence of the REF is negligible, with only a slight variation between 4K and 295K. In addition we find that correction of the resonance Raman profiles using the REF does not alter the results of the analysis or the conclusions presented in the main paper.

In addition we also present the reflectance contrast spectra comparing the WS_2 reflectivity and the silicon substrate at 4K Figure S6a which is dominated by the shift in the interference fringes due to WS_2 monolayer. The reflectance contrast spectrum comparing the WS_2 reflectivity at 4K and 295K Figure 6b however allows a peak associated with the A exciton to be observed.

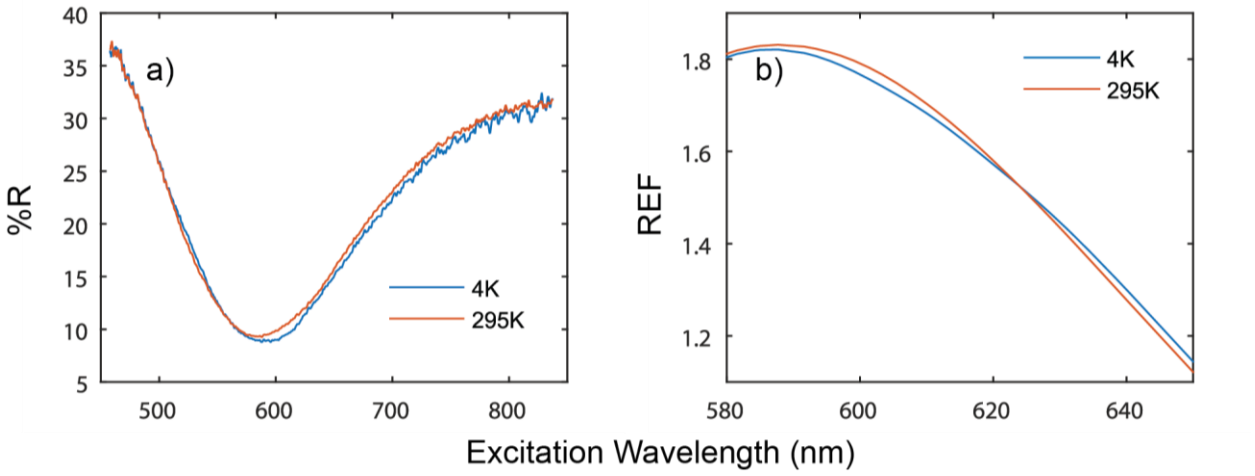

Figure S5 *a) Reflectivity spectra obtained on monolayer WS_2 at both 4K and 295K using a protected silver mirror as a reference. b) Raman enhancement factor determined from the reflectivity at 4K and 295K.*

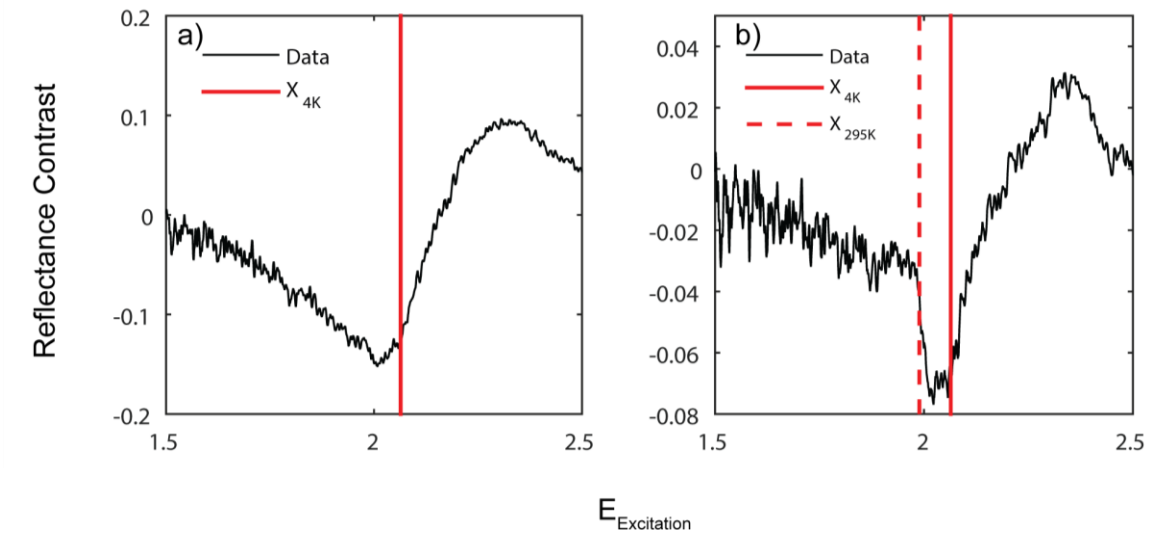

Figure S6 *a) Reflectance contrast spectra comparing the reflectivity of the WS_2 sample point S1 to the silicon substrate taken at 4K where the red line indicates the energy of the exciton at 4K. b) Reflectance contrast spectra comparing the reflectivity of the WS_2 on S1 at 4K and 295K with lines denoting the position of the exciton at 4K and 295K. Where reflectance contrast is defined as* $\frac{(R_{WS2}-R_{Substrate})}{(R_{WS2}+R_{Substrate})}$ *and* $\frac{(R_{4K}-R_{295K})}{(R_{4K}+R_{295K})}$ *for (a) and (b) respectively.*

Repeatability of Resonance Raman Measurements

In order to obtain the resonance Raman profiles it is necessary to ensure the repeatability of the Raman scattering intensities throughout the experiments. Due to the use of a tuneable laser source this requires careful alignment at each excitation wavelength to ensure the coupling of the Raman scattered light into the spectrometer is identical. We have previously presented the methods used for the resonance Raman measurements in Smith *et al.* [S8] which allows a repeatability of the Raman intensity of the order of 10%. The temperature dependent resonance Raman measurements were obtained over multiple experimental runs, with experiments carried out from 4K to 295K using both DCM and R6G laser dyes. During each experimental run multiple independent measurements were carried out at excitation energies of 1.97eV, 2.02eV, and 2.07eV, with repeat spectra for an experimental run shown in Figure S6. The repeat measurements were performed with an interval of 3-4 intermediate measurements at different excitation energies. The repeatability was then determined by fitting the A_1' peak and obtaining the Raman intensity. The average repeatability obtained for all temperatures and experimental runs was 9% ± 4%. This is comparable to the repeatability we have previously achieved for measurements on extreme nanowires presented in Spencer *et al.* [S9].

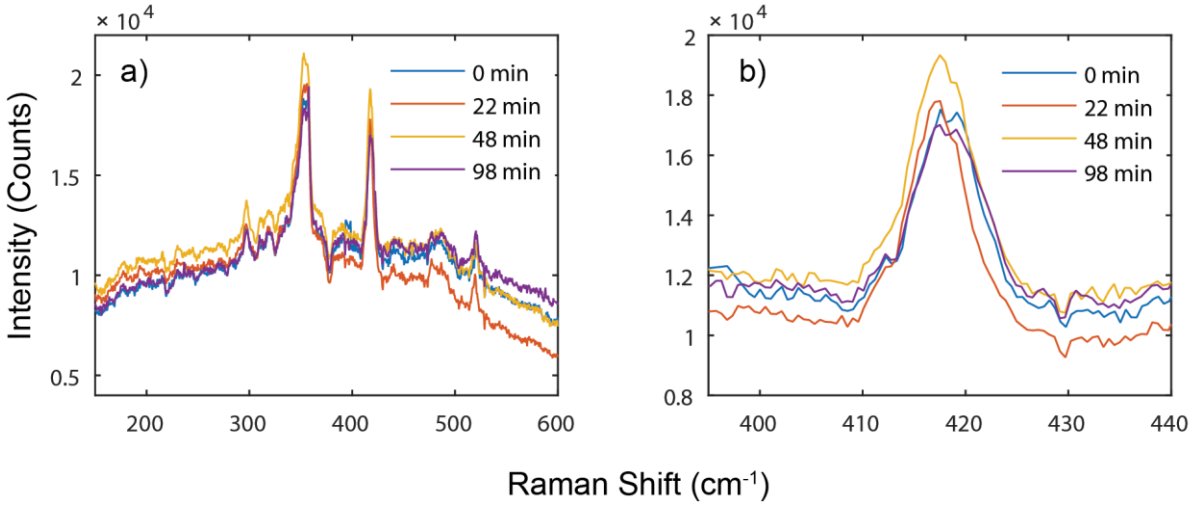

Figure S7 *(a) Repeat Raman spectra were taken at different times throughout the experimental run on monolayer WS_2 with an excitation wavelength of 600nm and at a temperature of 4K the time elapsed since the start of the experiment is included in the legend. The total duration for this experimental run was 142min. Panel (b) then provides an inset showing only the A_1' mode to fitting of the Raman peaks we obtain a repeatability of the Raman intensity of 9%.*

Fitted A_1' Resonance Profiles as a Function of Temperature

The amplitude coefficients, resonance widths and central energies extracted from the resonance profiles for the A_1' mode as a function of temperature were presented in the main paper. Here we present in Figure S8 the individual resonance profiles, with the obtained fits, for the A_1' mode from 4K to 295K. As discussed in the main text these have been fitted using the Raman scattering amplitude model for two electronic excitations with three scattering channels corresponding to exciton-exciton, trion-trion and exciton-trion scattering. In addition, we also present a comparison of the extracted exciton-trion scattering amplitude for the A_1' phonon as a function of temperature to the geometric average of the exciton-exciton, and trion-trion scattering amplitudes in Figure S9. The geometric average has been scaled by a factor of 3 to allow comparison of the temperature dependence. For both cases we find similar results with the strength of the exciton-trion scattering decreasing at higher temperatures. Although the associated errors are significant, so it is uncertain if the geometric average is in agreement with the exciton-trion scattering data.

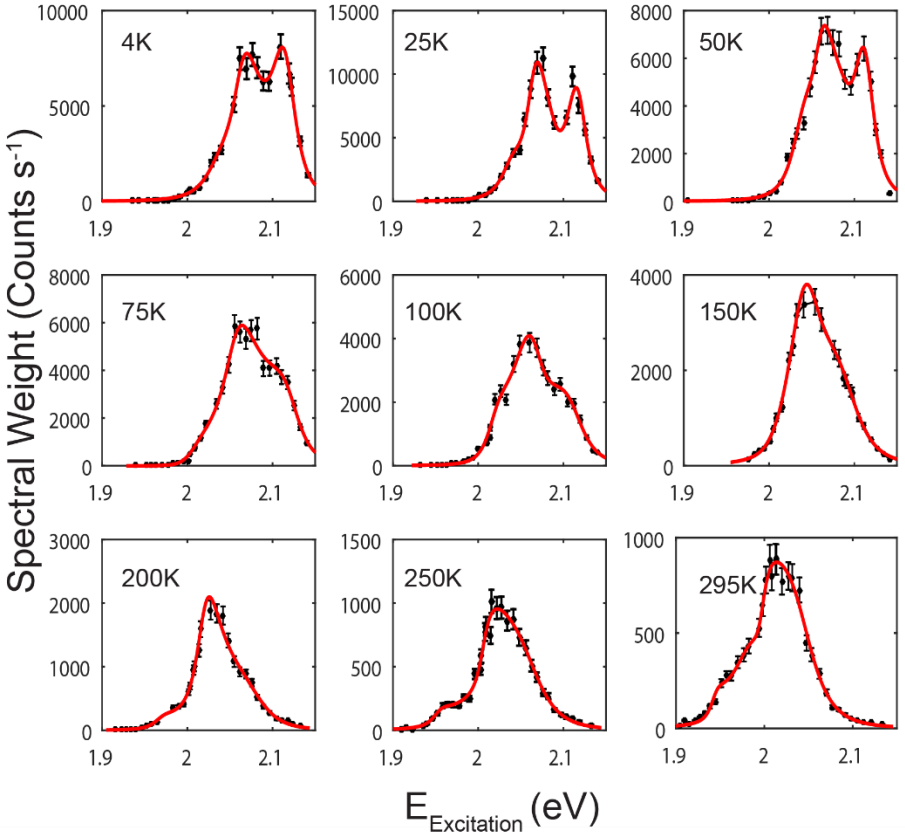

Figure S8 *Presents the fitted resonance Raman profiles for the A_1' mode as a function of temperature. In each case the fits have been obtained using two electronic excitations with scattering between electronic excitations and resulting in three Raman channels. Error bar shown are obtained from repeatability measurements during experimental runs.*

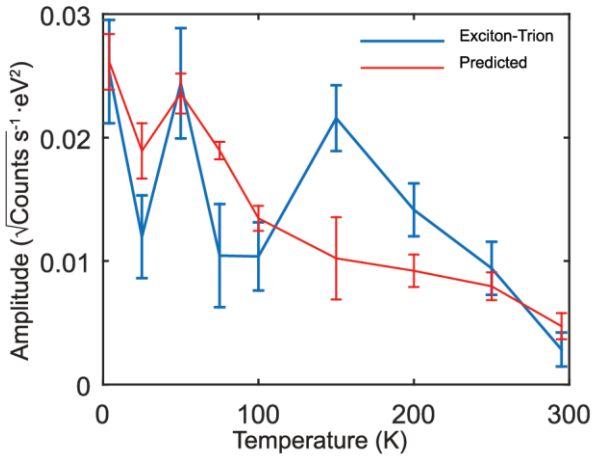

Figure S9 *Shows the fitted amplitude for the exciton-trion scattering channel with the predicted temperature dependence obtained from using the geometric average of the exciton-exciton, and trion-trion scattering amplitude coefficients.*

Comparison of resonance Raman profiles for all phonons at 4K

In order to facilitate the comparison of the resonance profiles presented in Fig 6 in the main manuscript, the fits and experimental data obtained for A_1', E', 2ZA, LA, 2LA, and Unassigned peak at 4K are presented in Figure S10 (a-b). For clarity we also present the fitted profiles separately from the data in Figure S10 (c-d).

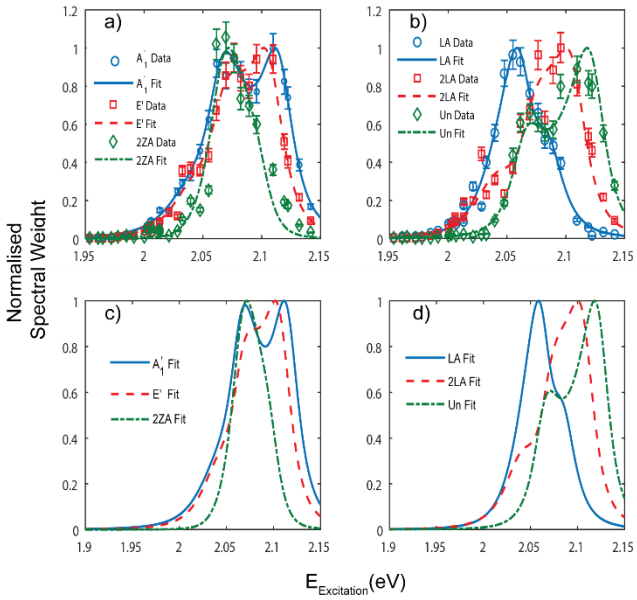

Figure S10 *Fits and experimental data for resonance Raman profiles at 4K for the single phonon peaks (a) and two phonon peaks (b) with error bars those obtained through repeatability measurements during experimental runs. In (c-d) we present only the fitted profiles to allow easy comparison of the difference in the shape of the resonance for different phonons.*

Photoluminescence Spectra

For completeness, we also present the photoluminescence spectra obtained at 4K and 295K Figure S11. These spectra were obtained using the same experimental setup as that for the Raman measurements with a 532nm laser diode. At 4K there is a clear peak centered at ~2.05eV which we associated with the exciton and trion emission and is in line with the energies obtained for these electronic excitations of 2.036eV and 2.064eV. In addition, the blue shift in the PL energy from 4K to 295K is ~ 60-70meV, which is in agreement with the observed shift of the electronic excitations presented in the main paper. There is also a lower energy contribution in the region <2eV and has been attributed in other PL measurements to localized states [S10].

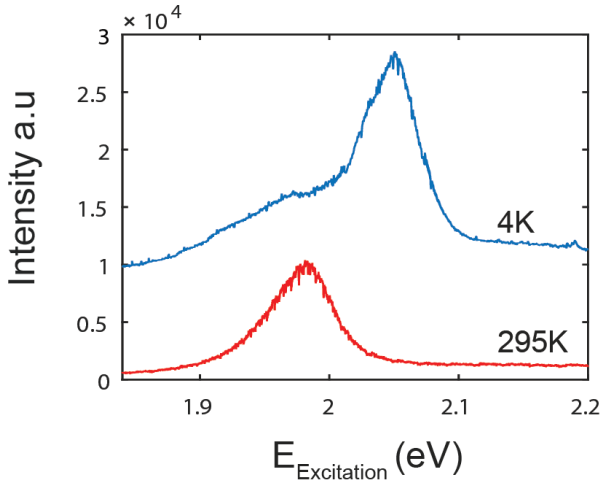

Figure S11 *Photoluminescence spectra obtained from monolayer WS_2 using a 532nm diode laser at 4K and 295K.*

Data Files

In addition two excel spreadsheets have been provided. The first contains the Raman spectra obtained from our experiments and the second contains data relating to the figures shown in the supplementary information, such as, reflectivity spectra, photoluminescence spectra, power linearity spectra, Anti-Stokes and Stokes Raman spectra. In each case the Raman spectra have been corrected for spectrometer efficiency. For a given temperature the data is contained within three separate spreadsheets For example the 4K data set will be contained in the spreadsheets labelled “4K Shift”, “4K Intensity”, and “4K WL”, which contain the Raman shift, intensity, and excitation wavelengths respectively. For the shift and intensity spreadsheets each column corresponds to an individual Raman spectra where the excitation wavelength used is given in the corresponding column in the wavelength spreadsheet.

References

(19) Berkdemir, A.; Gutiérrez, H. R.; Botello-Méndez, A. R.; Perea-López, N.; Elías, A. L.; Chia, C.-I.; Wang, B.; Crespi, V. H.; López-Urías, F.; Charlier, J.-C.; *et al.* Identification of Individual and Few Layers of WS_2 Using Raman Spectroscopy. *Sci. Rep.* **2013**, *3*, 1–8.

(27) Molina-Sánchez, a.; Wirtz, L. Phonons in Single-Layer and Few-Layer MoS_2 and WS_2. *Phys. Rev. B - Condens. Matter Mater. Phys.* **2011**, *84*, 1–8.

Supplementary References

(S1) Kip, B. J.; Meier, R. J. Determination of the Local Temperature at a Sample during Raman Experiments Using Stokes and Anti-Stokes Raman Bands. *Appl. Spectrosc.* **1990**, *44*, 707–711.

(S2) Maher, R. C.; Cohen, L. F.; Gallop, J. C.; Le Ru, E. C.; Etchegoin, P. G. Temperature-Dependent Anti-Stokes/stokes Ratios under Surface-Enhanced Raman Scattering Conditions. *J. Phys. Chem. B* **2006**, *110*, 6797–6803.

(S3) Yoon, D.; Moon, H.; Son, Y. W.; Choi, J. S.; Park, B. H.; Cha, Y. H.; Kim, Y. D.; Cheong, H. Interference Effect on Raman Spectrum of Graphene on SiO_2 /Si. *Phys. Rev. B - Condens. Matter Mater. Phys.* **2009**, *80*, 1–6.

(S4) Zhang, H.; Wan, Y.; Ma, Y.; Wang, W.; Wang, Y.; Dai, L. Interference Effect on Optical Signals of Monolayer MoS_2. *Appl. Phys. Lett.* **2015**, *107*, 101904.

(S5) Gao, L.; Lemarchand, R.; Lequime, M. Refractive Index Determination of SiO_2 Layer in the UV/Vis/NIR Range: Spectrophotometric Reverse Engineering on Single and Bi-Layer Designs. *J. Eur. Opt. Soc.* **2013**, *8*, 13010.

(S6) Aspnes, D. E.; Studna, a. a. Dielectric Functions and Optical Parameters of Si, Ge, GaP, GaAs, GaSb, InP, InAs, and InSb from 1.5 to 6.0 eV. *Phys. Rev. B* **1983**, *27*, 985–1009.

(S7) Li, Y.; Chernikov, A.; Zhang, X.; Rigosi, A.; Hill, H. M.; van der Zande, A. M.; Chenet, D. A.; Shih, E.-M.; Hone, J.; Heinz, T. F. Measurement of the Optical Dielectric Function of Monolayer Transition-Metal Dichalcogenides: MoS_2, $MoSe_2$, WS_2, and WSe_2. *Phys. Rev. B* **2014**, *90*, 205422.

(S8) Smith, D. C.; Spencer, J. H.; Sloan, J.; Mcdonnell, L. P.; Trewhitt, H.; Kashtiban, R. J.; Faulques, E. Resonance Raman Spectroscopy of Extreme Nanowires and Other 1D Systems 1 . Sample Preparation : Melt Filling of SWNTs with Mercury Telluride (HgTe) and Other. *J.Vis.Exp* **2016**, 1–14.

(S9) Spencer, J. H.; Smith, D. C.; McDonnell, L. P.; Sloan, J.; Kashtiban, R. J. Coherence Lifetime Broadened Optical Transitions in a 2 Atom Diameter HgTe Nanowire: A Temperature Dependent Resonance Raman Study. *RSC Adv.* **2016**, *6*, 95387–95395.

(S10) Plechinger, G.; Nagler, P.; Arora, A.; Granados Del Águila, A.; Ballottin, M. V.; Frank, T.; Steinleitner, P.; Gmitra, M.; Fabian, J.; Christianen, P. C. M.; *et al.* Excitonic Valley Effects in Monolayer WS_2 under High Magnetic Fields. *Nano Lett.* **2016**, *16*, 7899–7904.